Title: *In vivo* Raman spectroscopy for biochemical monitoring of the cervix throughout pregnancy

Authors: Christine M. O'BRIEN, PhD[1,2*], Elizabeth VARGIS, PhD[1,3*], Amy RUDIN, MSN[1], James C. SLAUGHTER, Dr. P.H. [4], Giju THOMAS, PhD[1,2], J Michael, NEWTON, MD[5], PhD, Jeff REESE, MD[2,6], Kelly A. BENNETT, MD[5], Anita MAHADEVAN-JANSEN, PhD[1,2,a]


1) Department of Biomedical Engineering, Vanderbilt University, Nashville, TN 37232
2) Biophotonics Center, Vanderbilt University, Nashville, TN 37232
3) Department of Biological Engineering, Utah State University, Logan, UT 84322
4) Department of Biostatistics, Vanderbilt University Medical Center, Nashville, TN 37232
5) Division of Maternal Fetal Medicine, Department of Obstetrics & Gynecology, Vanderbilt University Medical Center, Nashville, TN 37232
6) Division of Neonatology, Department of Pediatrics, Vanderbilt University Medical Center, Nashville, TN 37232

*Indicates co-first author.

The authors report no conflict of interest.

a) To whom correspondence should be addressed: Anita Mahadevan-Jansen, PO 351631 Station B, Nashville, TN 37235-1631 USA, 615-343-4787, anita.mahadevan-jansen@vanderbilt.edu

Abstract word count: 470
Main text word count: 4,052

One sentence condensation of the paper (25 words): *In vivo* Raman spectroscopy detects significant biochemical remodeling in the human cervix over the course of pregnancy and post-partum period

Short title: *In vivo* Raman spectroscopy detects significant biochemical remodeling in the human cervix over the course of pregnancy

Implications and Contributions (no more than 130 words): Raman spectra were non-invasively measured from the cervix of 68 women throughout the course of pregnancy and post-partum repair to monitor dynamic biomolecular profiles for improved understanding of cervical remodeling. Spectral analysis revealed significant decreases in contributions from extracellular matrix (ECM) proteins and significant increases in vascularity throughout the course of pregnancy. Parity and body mass index had significant effects on Raman spectra, and may help our understanding of adverse outcomes in delivery. This is the first report of Raman spectra measured from the cervix in pregnant women and the first study to non-invasively measure differences in the cervical biochemical environment based on patient factors. This work has high potential for translation and may aid understanding of premature cervical change in populations at high risk for preterm birth.

Abstract

BACKGROUND: The cervix must undergo significant biochemical remodeling to allow for successful parturition. This process is not fully understood, especially in instances of spontaneous preterm birth. *In vivo* Raman spectroscopy is an optical technique that can be used to investigate the biochemical composition of tissue longitudinally and non-invasively in humans, and has been utilized to measure physiology and disease states in a variety of medical applications.

OBJECTIVE: The purpose of this study is to measure *in vivo* Raman spectra of the cervix throughout pregnancy in women, and to identify biochemical markers that change with the preparation for delivery and post-partum repair.

STUDY DESIGN: Sixty-eight healthy pregnant women were recruited. Raman spectra were measured from the cervix of each patient monthly in the first and second trimesters, weekly in the third trimester, and at the six week post-partum visit. Raman spectra were measured using an *in vivo* Raman system with an optical fiber probe to excite the tissue with 785 nm light. A spectral model was developed to highlight spectral regions that undergo the most changes throughout pregnancy, which were subsequently used for identifying Raman peaks for further analysis. These peaks were analyzed longitudinally to determine if they underwent significant changes over the course of pregnancy ($p<0.05$). Finally, six individual components that comprise key biochemical constituents of the human cervix were measured to extract their contributions in spectral changes throughout pregnancy using a linear combination method. Patient factors including body mass index (BMI) and parity were included as variables in these analyses.

RESULTS: Raman peaks indicative of extracellular matrix proteins (1248, 1254cm$^{-1}$) significantly decreased ($p<0.05$), while peaks corresponding to blood (1233 and 1563 cm$^{-1}$)

significantly increased (p<0.0005) in a linear manner throughout pregnancy. In the post-partum cervix, significant increases in peaks corresponding to actin (1003, 1339, 1657 cm$^{-1}$) and cholesterol (1447 cm$^{-1}$) were observed when compared to late gestation, while signatures from blood significantly decreased. Post-partum actin signals were significantly higher than early pregnancy, whereas extracellular matrix (ECM) proteins and water signals were significantly lower than early weeks of gestation. Parity had a significant effect on blood and ECM protein signals, with nulliparous patients having significant increases in blood signals throughout pregnancy, and higher ECM protein signals in early pregnancy compared to patients with prior pregnancies. Body mass index significantly affected actin signal contribution, with low BMI patients showing decreasing actin contribution throughout pregnancy and high BMI patients demonstrating increasing actin signals.

CONCLUSION: Raman spectroscopy was successfully used to biochemically monitor cervical remodeling in pregnant women during prenatal visits. This foundational study has demonstrated sensitivity to known biochemical dynamics that occur during cervical remodeling, and identified patient variables that have significant effects on Raman spectra throughout pregnancy. Raman spectroscopy has the potential to improve our understanding of cervical maturation, and be used as a non-invasive preterm birth risk assessment tool to reduce the incidence, morbidity, and mortality caused by preterm birth.

Key words (alphabetized):

Cervical remodeling, in vivo, optical spectroscopy, post-partum, pregnancy, Raman spectroscopy

**Introduction**

Over half of all spontaneous preterm birth (sPTB) cases do not fall within any specific high-risk category, making the prediction and management of sPTB difficult [1]. While labor and parturition are coordinated processes involving many systems and organs for proper function, a full understanding of the cascade leading to labor and parturition has not been achieved, particularly in instances of sPTB. An arguably under-investigated but highly important organ for pregnancy maintenance and proper labor is the cervix, a dense extracellular matrix (ECM) that is infiltrated by cells, blood vessels, and smooth muscle [2,3]. The normal process of cervical remodeling that facilitates vaginal delivery occurs in four overlapping stages (softening, ripening, dilation, and repair) that have unique biochemical features and vary in duration among patients [4]. Furthermore, these processes are affected by patient factors including parity[5-8], prior vaginal delivery[9], and body mass index (BMI) [10-14].

Biochemically, the most abundant component of the ECM is fibrillar collagen, accounting for over 70% of the cervix tissue dry weight[9]. Other important ECM components include elastin, hyaluronan, sulfated glycosaminoglycans, proteoglycans, and water. During the softening phase, hydration and vascularity increase, remodeling the collagen matrix[4]. The ripening phase involves an accumulation of hydrophilic molecules including glycosaminoglycans such as hyaluronic acid, further increasing cervical tissue hydration. Additionally, collagen becomes increasingly soluble. While the total amount of collagen remains the same, the collagen concentration decreases due to an influx of water and other matrix constituents [15]. Next, cervical dilation occurs rapidly so the cervix can expand and dilate for delivery. Finally, during cervical repair, the collagen matrix of the cervix rebounds through an inflammatory process similar to wound healing[16,17], with an increase in macrophages and neutrophils that orchestrate ECM rebuilding[18].

Collagen remodeling occurs in all phases of cervical maturation, and has been identified as the most important contributor to the mechanical strength in the cervix [9,19]. A firm relationship has been established between the extent of collagen cross-linking and tensile strength in both the pregnant mouse [20] and human cervix tissues [21-23].

Researchers are working to develop new tools to quantitatively and non-invasively evaluate cervical remodelling *in vivo* to aid both basic understanding of the remodelling process and clinical decision-making. These methods include magnetic resonance, acoustic, mechanical, electrical, and optical techniques [24-26]. Light-based approaches can enable the study of tissue morphology and biochemistry depending on the light-tissue interaction process used. Two optical methods have been used *in vivo* to specifically monitor collagen. Fluorescence from collagen can be obtained by exciting tissue at ~340 nm. Previous studies have shown that fluorescence decreases over the course of pregnancy in mice and women [27-29]. Excitation at ~950 nm can produce an optical phenomenon termed second harmonic generation in collagen fibers, and can be used to create collagen-specific images that show well-defined collagen networks and ECM remodeling over the course of pregnancy [30,31].

Beyond collagen, near-infrared spectroscopy has been used to monitor other factors, including hydration, hemoglobin, and optical scatterers by measuring diffuse light scattering [32,33]. Absorption by hemoglobin and optical scattering were shown to increase hthroughout pregnancy, and absorption by water significantly increased during cervical ripening after exposure to the prostaglandin misoprostol [32,33]. Ectocervix surface area determined by images from an endoscopic camera reveal increased surface area in pregnant patients throughout pregnancy, and was attributed to increased hydration [34]. While fluorescence, second harmonic generation, near-infrared spectroscopy, and white light imaging have been applied *in vivo*, these methods provide

only a partial measure of the biochemical micro-environment. A single method that can probe hydration, proteins, and nuclear content as well as changes in vasculature could evaluate the role of each biomarker as well as the interplay between them during cervical remodeling.

Raman spectroscopy is an inelastic scattering technique that probes the vibrational energy levels of molecules. A Raman spectrum contains spectrally narrow peaks which are created by light interaction with distinct vibrational modes of molecules and therefore provides specific molecular fingerprints that are related to biochemistry and structure. Raman signals corresponding to lipids, proteins, saccharides, nucleic acids, and water, offer direct information regarding the biochemical makeup of the tissue, and signal intensity is linearly related to molecule concentration. Care must be taken during the interpretation of spectra in instances of peak overlap, such as the overlap of protein and water at 1657 cm$^{-1}$. In such cases, all Raman features of a given molecule must be analyzed, and spectral unmixing methods may be employed. Using Raman spectroscopy for direct understanding of molecular processes is difficult *in vivo* due to the large number of biochemical constituents that contribute to Raman spectra. Thus, *in vivo* information mainly provides relative abundance of biochemical constituents and in some cases structure which may be used to inform biology. Due to its high sensitivity and specificity, Raman spectroscopy has been increasingly used in biomedical applications [35], including detecting dysplasia in the human cervix [36-42]. In recent years, sensitivity to the hormonal status of cervical tissue has been seen in Raman spectra [43-45], which was the first step in using Raman spectroscopy to study cervical remodeling in mouse models of pregnancy [46,47]. Although mouse models allow for observation of pregnancy in a highly controlled manner, not all biology is conserved between mice and women, and clinical implementation introduces its own set of challenges.

The goal of this study is to test the feasibility of measuring Raman spectra of the *in vivo* cervix in pregnant women, and to characterize Raman signatures throughout pregnancy and post-partum. To this end, sixty-eight pregnant patients were enrolled in the study, and their cervices were measured throughout pregnancy and post-partum. Statistical analysis was performed longitudinally on the collected spectra, and highly significant changes in the spectra are observed as a function of gestation. In addition, patient factors including body mass index and obstetric history had significant effects on Raman spectra. To our knowledge, this is the first report using Raman spectroscopy to study cervical remodeling in pregnant women, demonstrating feasibility of the approach and identifying biochemical features associated with the phases of cervical remodeling.

**Materials and Methods**

Patient recruitment

This study was approved by the Vanderbilt University Medical Center's Institutional Review Board (#100544) and followed the guidelines of the Declaration of Helsinki. Pregnant patients receiving prenatal care at the Vanderbilt Women's Health Center were recruited using informed, written consent. To be eligible for enrollment, patients had to be at least 18 years old and able to provide legally valid prospective informed consent. Relevant patient information such as obstetric history, medications, age, BMI, and estimated date of delivery were all included in each patient's research chart. At the end of the study, patient outcome, delivery date and time were also recorded. Patient demographics are listed in Table 1. A total of 68 patients were enrolled in this study.

Experimental setup

A portable Raman spectroscopy system was used for data collection (Figure 1A). The system consists of a 785 nm diode laser (Innovative Photonics Solutions), an imaging spectrograph (Kaiser Holospec), a deep-depletion thermoelectrically cooled CCD camera (Princeton Instruments), a laptop computer, and a Raman spectroscopy fiber optic probe (EmVision LLC). The Raman probe (fiber optic probe approximately 2.1 mm in diameter, plus external stainless steel casing totaling 6.3 mm in outer diameter) consists of one optical fiber that transmits light from the laser to the tissue, surrounded by seven collection fibers that deliver the backscattered light to the spectrograph. The laser power at the sample was set to 80 mW.

Clinical protocol

After obtaining written, informed consent, the patient underwent a speculum exam performed by a certified Women's Health Nurse Practitioner. The cervix was exposed and cleaned with a cotton swab soaked in sterile saline before the Raman probe was gently placed in contact with the cervix to obtain a Raman spectrum (Figure 1B). The overhead room lights were turned off, and 3-5 measurements were taken from separate locations around the ectocervix, taking care to ensure that the probe was placed on the squamous epithelium. Each measurement used an integration time of 3 seconds, and the entire process took less than 10 minutes per visit. The Raman probe was disinfected after each patient in accordance with standard disinfection procedures. For each patient, spectra were acquired monthly in the first and second trimester, weekly in the third trimester, and at six week post-partum.

Data processing

Each day, the Raman spectroscopy system was wavelength calibrated using a Neon Argon lamp. The exact laser excitation wavelength and Raman shift were calculated using acetaminophen and naphthalene standards which have well characterized Raman shifts. The spectral response of the system was first determined using a NIST calibrated tungsten lamp, and then calibrated daily using a piece of green glass that has a similar broadband spectrum. The resultant calibration factor was applied to each spectrum based on the spectral throughput measured each day. Raman spectra were processed to remove ambient background light, noise smoothed using a Savitsky-Golay filter, and fluorescence subtracted using the modified polynomial method [48].

Data analysis

In order to determine how the average Raman spectrum changes over the course of pregnancy and post-partum, a restricted cubic spline function for Raman shift (cm$^{-1}$) with "k degrees of freedom" or "k-1 knots", where k was set to 65. Sixty-five knots were chosen in order to minimize the number of variables in the model without sacrificing spectral information. Additional patient variables, including prior vaginal delivery and BMI were incorporated as continuous variables in this spectral model, resulting in a series of Raman spectra representative of various stages of pregnancy and post-partum.

Spectral regions that appeared to change throughout pregnancy based on observations from the spectral model were used for calculating changes in Raman peaks and Raman peak ratios over pregnancy. Peak ratio calculations provide data normalization and thus allow improved comparison across datasets with varying signal to noise ratios. Using this approach, the following peaks were identified for further analysis: 1006, 1055, 1125, 1157, 1248, 1254, 1304,

1339, 1451, 1563, and 1657 cm$^{-1}$. To determine whether peak or peak ratio intensities changed as the cervix prepared for delivery, generalized estimating equations[49,50] (GEEs, a type of linear model that clusters data obtained from each patient over time in order to account for the inherent correlation between measurements from the same patient) were developed for longitudinal monitoring. The change in each peak or peak ratio over time was modeled and plotted with its mean and its 95% confidence interval based on the GEE output, and ANOVA was performed on the model output to determine statistical significance (* indicates $p < 0.05$ over the course of pregnancy). GEE output plots enable the analysis of cervical remodeling as a continuous variable, such that the not only the spectral peak levels can be observed in each trimester, but also the rate of change within, between, and throughout all trimesters. Next, major biochemical contributors to the Raman spectra were tracked throughout pregnancy and post-partum using a biochemical model termed non-negative least squares (NNLS) analysis. Pure components known to be present in the cervix were measured and the tissue spectrum was recreated using a linear combination of the pure components. The components used for the model were measured in their pure form and include actin, adenosine triphosphate, cholesterol, collagen type I, deoxyribonucleic acid, glucose, glycogen, phosphatidylcholine, phosphatidylethanolamine, progesterone, and prostaglandin $E_2$ (Sigma, St. Louis, MO), glucose-6-phosphate (Roche Diagnostics GmbH, Mannheim, Germany), hyaluronic acid (Abcam, Cambridge, MA), blood (excess human blood from use in IRB-approved protocol #151532), and deionized water. All measurements were acquired using the same integration time and are displayed in Supplemental Figure 1.

Non-negative least squares analysis is most accurate when non-correlated spectral components are used in the model; therefore the correlation coefficient between each

biochemical signal was calculated (Supplemental Figure 2). If any two biochemical components had a Spearman correlation coefficient higher than 0.75, one of the two components was chosen to be input for the model and the other was not included. The model was computed using MATLAB. The pure component spectra were loaded into a matrix with each column containing a pure component spectrum. Patient spectra were input to the model and the best fit coefficients from each component were calculated. In addition, the residual between the model fit and the tissue spectrum was calculated to ensure all regions of the Raman spectra were adequately represented.

To longitudinally monitor how each biochemical molecule changed throughout pregnancy, the biochemical coefficients were analyzed using GEEs as explained above. In addition, patient variables including obstetric history (parity) and BMI were incorporated into the model as continuous variables to determine their effects on Raman spectra throughout pregnancy. Studies have shown that BMI and parity have an influence on the ability of Raman Spectroscopy to correctly characterize cervical spectra [51], and are factors that contribute to the timing of parturition [10,11,14].

## **Results**

### Spectral changes throughout pregnancy

Raman spectra collected throughout pregnancy changed significantly as the cervix prepared for delivery. Representative spectra from one patient measured throughout her pregnancy and post-partum are shown in Figure 1C. Multiple regions show considerable variation including 1030-1100 $cm^{-1}$, 1118-1200 $cm^{-1}$, 1230-1260 $cm^{-1}$, 1270-1330 $cm^{-1}$, 1440-1460 $cm^{-1}$, 1550-1600 $cm^{-1}$, and 1630-1670 $cm^{-1}$. The post-partum spectrum is particularly

distinct from the prenatal measurements, and most closely resembles the earliest measurement obtained at the patient's 8 week prenatal visit. However significant increases in the 1118-1200, 1300-1350, and 1630-1670 cm$^{-1}$ regions are observed, unique to the post-partum period.

The spectral model, which was developed to determine the average Raman spectra over the course of pregnancy for the entire patient population studied, is shown in Figure 2. Several significant changes were observed over pregnancy and post-partum, which are highlighted by the gray shaded regions in Figure 2 (* indicates significant change over the course of pregnancy with $p<0.05$). The 1530-1600 cm$^{-1}$ region attributed to peaks observed in blood (as seen in Figure 4B) increases with advancing gestation, whereas bands characteristic of ECM proteins (as observed in the collagen spectrum in Figure 4C) (1030-1100 cm$^{-1}$, 1230-1290 cm$^{-1}$, 1440-1460 cm$^{-1}$, and 1630-1670 cm$^{-1}$) and carotenoids (1130-1200 cm$^{-1}$) decrease throughout pregnancy. In addition, the left shoulder of the 1657 cm$^{-1}$ peak appears to increase (Figure 2). Post-partum, bands observed in ECM proteins return to early pregnancy levels and there is significantly higher intensity in the 1270-1330 cm$^{-1}$ range. Although Figure 2 depicts a computational representation of the data, the majority of the spectral changes that occurred throughout gestation are seen in the example patient spectra in Figure 1C, demonstrating the utility and accuracy of the model.

Several peaks undergo significant changes over the course of pregnancy (* indicates $p<0.05$), including peaks at 1157, 1248, and 1254 cm$^{-1}$ which significantly decrease throughout pregnancy, and the 1563 cm$^{-1}$ peak which significantly increases as a function of gestation week (Supplemental Figure 3). Post-partum measurements are significantly higher ($p<0.05$) in the 1304 and 1339 cm$^{-1}$ peaks compared to early pregnancy (<22 weeks of gestation), and significantly lower in the 1006 and 1657 cm$^{-1}$ peaks. A similar comparison of post-partum spectra to those taken at the end of gestation (>37 weeks) reveals significantly higher intensities

post-partum at 1248, 1254, and 1339 cm$^{-1}$, and significantly lower intensities in the 1006, 1563, and 1657 cm$^{-1}$. Raman peak ratio calculations reveal many features that change significantly throughout pregnancy and post-partum (Figure 3), including the 1254/1304 cm$^{-1}$ ratio (ECM protein to actin & glycogen ratio) which decreases as term approaches ($p<0.0001$), and is significantly lower post-partum compared to early pregnancy (Figure 3A). In addition, the 1563/1248 cm$^{-1}$ peak ratio (blood to ECM protein ratio) steadily increases over gestation ($p<0.0001$), and post-partum measurements are significantly lower than late pregnancy (Figure 3B). The 1157/1339 cm$^{-1}$ peak ratio (carotenoid to ECM protein ratio) significantly decreases throughout gestation until term ($p<0.005$), and post-partum measurements are significantly lower than early pregnancy (Figure 3C).

Raman spectra of purified biochemical components

Six biochemical components were used to construct the least squares model (actin, blood, cholesterol, collagen I, glycogen, and water), and their Raman spectra are depicted in Figure 4A-F. These spectra showcase the specificity of Raman spectroscopy to different types of biomolecules. An example of an *in vivo* spectrum obtained from cervical tissue, overlaid with its least squares fit and resulting residual are displayed in Figure 4G. The residual is small and fluctuates above and below zero, with an $R^2$ value of 0.922, indicative of a good fit.

The contributions of two biochemical components change significantly as a function of gestation (* indicates $p<0.05$), as shown in Figure 5. The contribution from blood significantly increases in a linear manner ($p<0.0005$), whereas the contribution from collagen decreases over the course of pregnancy ($p<0.0001$). Comparing post-partum measurements to early pregnancy (<22 weeks of gestation) reveal significantly higher ($p<0.05$) post-partum levels of actin, and a

significantly lower contributions from collagen type I and water. Additionally, comparison of post-partum to the end of gestation (>37 weeks of gestation) reveals significantly higher actin and cholesterol contribution, and significantly lower blood contribution in the post-partum fits.


Effects of patient variables

While several patient variables were considered, parity and BMI were found to have an effect on Raman spectra during pregnancy and post-partum (Figure 6). From NNLS analysis blood/vascularity signals have an inverse relationship with parity, with nulliparous patients showing significant increases in blood/vascularity signals as the cervix remodels, compared with a relatively stable blood contribution in parous patients (Figure 6A, Supplemental Figure 4A) ($p<0.05$). Individual peak analysis reveals that the 1125 cm$^{-1}$ peak increases steadily in nulliparous patients, but does not increase until about 30 weeks of gestation in parous patients (Supplemental Figure 4B). Additionally, the 1254 cm$^{-1}$ peak is significantly higher at the beginning of pregnancy and significantly lower near term in nulliparous patients, although parous patients do show decreases in this peak throughout pregnancy (Supplemental Figure 4C). Post-partum, parous patients had significantly higher contributions from cholesterol (Supplemental Figure 4D), while nulliparous patients had significantly higher intensities at 1006 (Supplemental Figure 4E) and 1055 cm$^{-1}$ (possibly caused by ECM proteins or actin) (Supplemental Figure 4F) than parous patients.

Evaluation of the effects of BMI shows that low BMI patients (demonstrated by spectral model with BMI=25) have decreasing actin contributions as the cervix prepares for delivery ($p<0.05$) which levels outs as BMI increases (Supplemental Figure 5A). In addition, low BMI patients start with higher signal from 1248 cm$^{-1}$, a peak characteristic of ECM proteins, but

decreases to a greater extent than high BMI patients at term (Supplemental Figure 5B). Post-partum spectra from low BMI patients have higher actin contribution and higher 1003 cm$^{-1}$ peak intensity compared to high BMI patients (demonstrated by model with BMI=40 in Figure 6 and in Supplemental Figure 5A&C). In addition, high BMI patients have higher contribution from collagen than low BMI patients in the post-partum period (Supplemental Figure 4D).


**<u>Comment</u>**

Monitoring the cervix during pregnancy has many purposes; these include improved understanding of normal and abnormal physiology of cervical remodeling, estimating delivery time, and determining patient readiness for labor. This last clinical task is currently conducted using the Bishop Score and in some cases ultrasound; however these methods provide limited information, mainly pertaining to cervical structure. In this study, Raman spectroscopy was employed to non-invasively measure the biochemistry of the cervix over the course of pregnancy *in vivo* in women for the first time. This approach successfully measured known biochemical changes observed in  multiple stages of pregnancy and post-partum repair, and established patient variables that affect the remodeling process, demonstrating the utility of Raman spectroscopy for cervical evaluation during pregnancy.

*In vivo* Raman measurements of the cervix acquired over the course of pregnancy revealed characteristic biochemical changes that occur in preparation for delivery. Decreases in peaks indicative of extracellular matrix proteins such as collagen (1055, 1248, and 1657 cm$^{-1}$) and increases in peaks corresponding to blood (1233 and 1563 cm$^{-1}$) are observed in the example patient spectra (Figure 1C), the spectral model determined from 68 patients (Figure 2), and the non-negative least squares analysis (Figure 5). An increase in blood signatures is attributed to the

increase in vascularization that occurs as the cervix prepares for delivery [4] (Figure 5), a phenomenon which has also been observed in pregnant women using near infrared spectroscopy[33]. Decreases in ECM peaks are explained by the process of ECM remodeling where collagen becomes increasingly soluble due to reduced cross-links and dispersed at a lower concentration [4,15]. Trivalent collagen cross-links have been observed at 1660 cm$^{-1}$, and reductions in these cross-links (which have been previously reported in women[27] and mice[27,52]) likely contribute to the observed decrease in this peak during pregnancy[53]. Furthermore, the 1657 cm$^{-1}$ peak (also known as the amide I region) broadened in preparation for delivery, a phenomenon that is known to be caused by structural disorder such as collagen fiber dispersion [54]. This broadening may also be attributed to increased blood signals which have a peak at 1619 cm$^{-1}$. In pregnant women, collagen solubility has been measured *in vivo* using laser-induced fluorescence where fluorescent intensity corresponding to collagen cross-links was shown to decrease throughout pregnancy[28]. Fiber dispersion has been measured during pregnancy *ex vivo* in mice and women using second harmonic generation[55] and optical coherence tomography[56]. An increase in collagen fiber dispersion was seen using both techniques. In the post-partum cervix, Raman spectral signatures were significantly different from measurements obtained during pregnancy, with increases in spectral features corresponding to actin and cholesterol, and decreases in features corresponding to blood, collagen type I, and water as observed in Figure 5. There are few studies focused on understanding post-partum repair, however these studies suggest that the repair process is governed by immune cells which infiltrate the cervix and create a proinflammatory environment that resembles wound healing [18,57,58]. Microarray studies have found that in addition to inflammatory genes, matrix synthesis and collagen strengthening genes are upregulated in the post-partum cervix [16,17]. Based on this evidence, it is possible that the

spectral increases of actin and cholesterol are caused by an influx of immune cells and fibroblasts. Although post-partum contributions from glycogen did not reach statistical significance due to variability in measurement time point (2-12 weeks post-partum), a possible explanation for the observed heightened glycogen levels is intensive anabolic activity driving the repair process. Furthermore, the peak at 1160 cm$^{-1}$ is found in many carotenoid antioxidants [59-61] which could be elevated post-partum to combat high levels of reactive oxygen species related to macrophages and neutrophil infiltration.

Two patient variables, parity and body mass index, affected spectral changes that were observed throughout pregnancy and post-partum (Figure 6). Nulliparous patients started pregnancy with higher spectral contributions from collagen (based on the NNLS model) compared to parous (Figure 6A). In fact, this observation is supported by an *ex vivo* study in which collagen concentration (determined via hydroxyproline assay) was measured from cervical biopsies taken from parous and nulliparous women, and revealed decreasing collagen levels as parity increased [8]. These findings were corroborated with *ex vivo* biomechanical tests of non-pregnant tissues from patients with and without prior vaginal deliveries which revealed stiffer, less compliant tissue in patients without prior vaginal deliveries [9], and confirmed decreased collagen extractability, as well as increased sulfated glycosaminoglycans and hydration in patients with a history of prior vaginal delivery. It is likely that a permanent vascular network is established during the first pregnancy similar to permanent changes in mechanical properties[9], which would explain why patients with prior pregnancies had significantly higher baseline blood/vascularity levels compared to nulliparous patients. Taken together, these results are unsurprising, as multiparous patients generally have faster labors [5-7], indicating that some level

18

of permanent cervical remodeling occurs after completing all four phases of cervical remodeling during a prior pregnancy.

Patients with low BMI have higher spectral signals corresponding to ECM proteins (1248 cm$^{-1}$ peak) at the beginning of pregnancy (Figure 6B), but this intensity decreases significantly more than high BMI patients by term, indicating that high BMI patients experience a lesserr level of ECM remodeling. One possible explanation for this observation is an increase in leptin, an adipokine that is elevated in pregnant patients with high BMI, which has been shown to disrupt MMP action on collagen in myometrial tissues and synthesize myometrial collagen in late pregnancy [14,62,63]. It is possible that this phenomenon also occurs in the cervix, reducing the extent of cervical remodeling achieved, and contributing to extended labor times and increased C-section rates observed in high BMI (>30) patients [10-14]. In addition, actin signals decreased throughout pregnancy in low BMI patients, possibly caused by cervical cell apoptosis which occurs prior to labor [17]. However, actin signals did not decrease in high BMI patients, which may also be attributed to high leptin levels which have been shown to prevent cell apoptosis *in vitro* [14,64].

Nine of the patients enrolled in the present study underwent preterm birth, ranging from 35 + 3/7 weeks to 36 +6/7 weeks gestation when they delivered. Analysis was performed to determine if any differences were observed in this data set compared to patients who delivered at term, but none reached statistical significance. This result is not surprising, as these patients had different obstetric histories, body mass indexes, and all delivered relatively close to term. For a powered analysis comparing patients with and without PTB, additional studies that specifically enroll a large number of high risk patients will be required.

Although not yet ready for the launch of a clinical tool, it is important to think about how such a tool would be used and incorporated into the current workflow. The long term goals include the ability to measure premature cervical change at the patient bedside, as well as determine the etiology of the changes measured. The authors envision that Raman measurements could be made from the cervix early in pregnancy such as at the first appointment to obtain a baseline measurement. The frequency with which measurements would need to be made has not yet been established, and will likely require studies that evaluate the cost-benefit analysis of a variety of frequencies. Short term, Raman measurements could be introduced as an additional test for assessment of premature cervical change and ideally provide clues pointing towards the etiology. It is also unclear whether data will need to be normalized to a previous measurement taken from the patient, or whether a single measurement could provide enough information to determine premature cervical change. Advanced predictive algorithms will need to be developed, first indicating abnormal spectral profiles, and then hopefully indicating abnormal changes with information regarding etiology. Based on results in this study, variables including parity and body mass index will need to be incorporated into the algorithms. In addition to use as a PTB risk assessment tool, Raman spectroscopy could be used to aid our biological understanding of problems such as cervical insufficiency, ascending infection, and monitoring efficacy of new treatment strategies for preterm labor.

Limitations of this study include the need for validation of the Raman spectral findings. Investigation in mouse pregnancy is underway[46,47] which has the ability to validate *in vivo* findings from Raman spectra, and future study of patients undergoing hysterectomy will provide additional opportunity to compare *in vivo* Raman spectra to *ex vivo* biochemical assays. In addition, interpretation of Raman spectra can be difficult due to the overlap of many spectral

features in biological samples and changes in structure rather than concentration. Although Raman spectral intensity and vibrational mode concentration are linear, multiple biochemical components may include the same vibrational mode such as C-H stretch found in organic molecules. Observing the full spectrum can aid in these cases as distinguishing features likely exist between different biomolecules. When using Raman spectroscopy as a biological tool, it is important to remember that Raman spectra yield a relative concentration of biochemical species comprising tissue at the time of measurement. This information can help in understanding of the current microenvironment, but its use for determining molecular function or understanding mechanisms of molecular processes is challenging *in vivo* due to the nature of high overlap from thousands of biomolecules. Lastly, in this study, the Raman spectra are not depth-resolved, and therefore comment cannot be made regarding whether the biochemical signals originated from the cervical epithelium or stroma. For example, it is currently not possible to determine whether actin signals originated from epithelial cells or fibroblasts and smooth muscle cells deep in the cervical stroma. Raman probes can be developed that allow this capability and may be employed in future studies. The main strength of this study lies in the ability to monitor multiple dynamic biochemical changes in the cervix as it remodels to deliver the fetus. Although other optical modalities are sensitive to certain biochemical components such as collagen or blood, Raman spectroscopy provides simultaneous monitoring of ECM proteins, lipids, blood, saccharides, antioxidants, and metabolic enzymes without the addition of exogenous labels or removal of tissue. This technique has high potential for better understanding the etiologies and progression of spontaneous preterm birth, and may also help to unveil the healing process that occurs during post-partum repair. Translation of Raman spectroscopy to clinical settings is becoming more realistic each year; real-time data processing has already been achieved [65,66], and fully

characterized disease and/or physiology profiles allow for automation of data analysis and tissue classification at the bedside. Hardware advances are consistently moving forward, which promise to reduce complexity of the system [35]. These studies also bring us closer to identifying a spectral signature that defines cervical changes in normal pregnancy, increasing the potential to utilize Raman spectroscopy for predicting the timing of delivery and therefore early risk assessment for preterm birth.

In summary, this study highlights Raman spectroscopy as a tool to track meaningful chemical signals in cervical tissue throughout pregnancy and during post-partum repair. This is the first study to demonstrate the utility of Raman spectroscopy as a basic research tool in obstetrics via its sensitivity to known dynamic biochemical changes that occur during cervical remodeling, and marking an important step towards development of a clinical tool. With continued advancement, Raman spectroscopy has the potential to improve patient care by arming providers with information on the biochemical state of the cervix, close gaps in our understanding of cervical maturation, and identify women at risk for preterm birth.

References

1. Macdonald PC, Gant NF, Leveno KJ, Gilstrap LC, Hankins G, Clark SL. *Williams Obstetrics 20th Edition.* Appleton & Lange; 1996.
2. Ludmir J, Sehdev HM. Anatomy and physiology of the uterine cervix. *Clinical Obstetrics and Gynecology.* 2000;43(3):433-439.
3. Vink JY, Qin S, Brock CO, et al. A new paradigm for the role of smooth muscle cells in the human cervix. *Am J Obstet Gynecol.* 2016;215(4):478.e471-478.e411.
4. Word RA, Li XH, Hnat M, Carrick K. Dynamics of cervical remodeling during pregnancy and parturition: mechanisms and current concepts. *Semin Reprod Med.* 2007;25.
5. Friedman EA, Kroll BH. Computer analysis of labor progression. 3. Pattern variations by parity. *J Reprod Med.* 1971;6(4):179-183.
6. Vahratian A, Hoffman MK, Troendle JF, Zhang J. The impact of parity on course of labor in a contemporary population. *Birth.* 2006;33(1):12-17.
7. Harper LM, Caughey AB, Odibo AO, Roehl KA, Zhao Q, Cahill AG. Normal progress of induced labor. *Obstet Gynecol.* 2012;119(6):1113-1118.
8. Petersen LK, Uldbjerg N. Cervical collagen in non-pregnant women with previous cervical incompetence. *Eur J Obstet Gynecol Reprod Biol.* 1996;67(1):41-45.
9. Myers KM, Paskaleva A, House M, Socrate S. Mechanical and biochemical properties of human cervical tissue. *Acta Biomaterialia.* 2008;4(1):104-116.
10. Ovesen P, Rasmussen S, Kesmodel U. Effect of prepregnancy maternal overweight and obesity on pregnancy outcome. *Obstet Gynecol.* 2011;118(2 Pt 1):305-312.
11. Vahratian A, Zhang J, Troendle JF, Savitz DA, Siega-Riz AM. Maternal prepregnancy overweight and obesity and the pattern of labor progression in term nulliparous women. *Obstet Gynecol.* 2004;104.
12. Gauthier T, Mazeau S, Dalmay F, et al. Obesity and cervical ripening failure risk. *The journal of maternal-fetal & neonatal medicine : the official journal of the European Association of Perinatal Medicine, the Federation of Asia and Oceania Perinatal Societies, the International Society of Perinatal Obstet.* 2012;25(3):304-307.
13. Lassiter JR, Holliday N, Lewis DF, Mulekar M, Abshire J, Brocato B. Induction of labor with an unfavorable cervix: how does BMI affect success? *The Journal of Maternal-Fetal & Neonatal Medicine.* 2016;29(18):3000-3002.
14. Carlson NS, Hernandez TL, Hurt KJ. Parturition dysfunction in obesity: time to target the pathobiology. *Reproductive Biology and Endocrinology.* 2015;13(1):135.
15. Leppert PC. Anatomy and physiology of cervical ripening. *Clinical Obstetrics and Gynecology.* 1995;38(2):267-279.
16. Timmons BC, Mahendroo M. Processes regulating cervical ripening differ from cervical dilation and postpartum repair: insights from gene expression studies. *Reproductive sciences (Thousand Oaks, Calif).* 2007;14(8 Suppl):53-62.
17. Hassan SS, Romero R, Haddad R, Hendler I, Khalek N, Tromp G. The transcriptome of the uterine cervix before and after spontaneous term parturition. *Am J Obstet Gynecol.* 2006;195.
18. Timmons BC, Fairhurst AM, Mahendroo MS. Temporal changes in myeloid cells in the cervix during pregnancy and parturition. *J Immunol.* 2009;182(5):2700-2707.
19. House M, Kaplan DL, Socrate S. Relationships Between Mechanical Properties and Extracellular Matrix Constituents of the Cervical Stroma During Pregnancy. *Seminars in Perinatology.* 2009;33(5):300-307.

20. Akins ML, Luby-Phelps K, Bank RA, Mahendroo M. Cervical softening during pregnancy: regulated changes in collagen cross-linking and composition of matricellular proteins in the mouse. *Biology of Reproduction.* 2011;84(5):1053-1062.

21. Rechberger T, Uldbjerg N, Oxlund H. Connective tissue changes in the cervix during normal pregnancy and pregnancy complicated by cervical incompetence. *Obstet Gynecol.* 1988;71(4):563-567.

22. Myers KM, Socrate S, Paskaleva A, House M. A study of the anisotropy and tension/compression behavior of human cervical tissue. *Journal of Biomechanical Engineering.* 2010;132(2):021003-021003.

23. Myers K, Socrate S, Tzeranis D, House M. Changes in the biochemical constituents and morphologic appearance of the human cervical stroma during pregnancy. *European Journal of Obstetrics & Gynecology and Reproductive Biology.* 2009;144:S82-S89.

24. Feltovich H, Hall TJ, Berghella V. Beyond cervical length: emerging technologies for assessing the pregnant cervix. *American Journal of Obstetrics and Gynecology.* 2012;207(5):345-354.

25. O'Brien CM, Vargis E, Paria BC, Bennett KA, Mahadevan-Jansen A, Reese J. Raman spectroscopy provides a noninvasive approach for determining biochemical composition of the pregnant cervix in vivo. *Acta Paediatr.* 2014;103(7):715-721.

26. Hee L. Overview of the methods available for biomechanical testing of the uterine cervix in vivo. *Acta Obstet Gynecol Scand.* 2014;93(12):1219-1237.

27. Maul H, Saade G, Garfield RE. Prediction of term and preterm parturition and treatment monitoring by measurement of cervical cross-linked collagen using light-induced fluorescence. *Acta Obstetricia et Gynecologica Scandinavica.* 2005;84(6):534-536.

28. Maul H, Olson G, Fittkow CT, Saade GR, Garfield RE. Cervical light-induced fluorescence in humans decreases throughout gestation and before delivery: preliminary observations. *American Journal of Obstetrics and Gynecology.* 2003;188(2):537-541.

29. Schlembach D, MacKay L, Shi L, Maner WL, Garfield RE, Maul H. Cervical ripening and insufficiency: From biochemical and molecular studies to in vivo clinical examination. *European Journal of Obstetrics &amp; Gynecology and Reproductive Biology.* 2009;144, Supplement 1(0):S70-S76.

30. Zhang Y, Akins ML, Murari K, et al. A compact fiber-optic SHG scanning endomicroscope and its application to visualize cervical remodeling during pregnancy. *Proceedings of the National Academy of Sciences.* 2012;109(32):12878-12883.

31. Reusch LM, Feltovich H, Carlson LC, et al. Nonlinear optical microscopy and ultrasound imaging of human cervical structure. *Journal of Biomedical Optics.* 2013;18(3):031110-031110.

32. Baños A, Wolf M, Grawe C, et al. Frequency domain near-infrared spectroscopy of the uterine cervix during cervical ripening. *Lasers in Surgery and Medicine.* 2007;39(8):641-646.

33. Hornung R, Spichtig S, Baños A, Stahel M, Zimmermann R, Wolf M. Frequency-domain near-infrared spectroscopy of the uterine cervix during regular pregnancies. *Lasers in medical science.* 2011;26(2):205-212.

34. Qian X, Jiang Y, Liu L, Shi SQ, Garfield RE, Liu H. Changes in ectocervical surface area in women throughout pregnancy compared to non-pregnant and postpartum states. *The journal of maternal-fetal & neonatal medicine : the official journal of the European Association of Perinatal Medicine, the Federation of Asia and Oceania Perinatal Societies, the International Society of Perinatal Obstet.* 2016;29(22):3677-3681.

35. Pence I, Mahadevan-Jansen A. Clinical instrumentation and applications of Raman spectroscopy. *Chemical Society reviews.* 2016;45(7):1958-1979.

36. Mo J, Zheng W, Low JJ, Ng J, Ilancheran A, Huang Z. High wavenumber Raman spectroscopy for in vivo detection of cervical dysplasia. *Analytical Chemistry-Columbus.* 2009;81(21):8908.

37. Duraipandian S, Zheng W, Ng J, Low JJ, Ilancheran A, Huang Z. In vivo diagnosis of cervical precancer using Raman spectroscopy and genetic algorithm techniques. *Analyst.* 2011;136(20):4328-4336.

38. Duraipandian S, Zheng W, Ng J, Low JJ, Ilancheran A, Huang Z. Simultaneous fingerprint and high-wavenumber confocal raman spectroscopy enhances early detection of cervical precancer in vivo. *Analytical chemistry.* 2012;84(14):5913-5919.

39. Lyng FM, Faoláin EÓ, Conroy J, et al. Vibrational spectroscopy for cervical cancer pathology, from biochemical analysis to diagnostic tool. *Experimental and Molecular Pathology.* 2007;82(2):121-129.

40. Krishna CM, Prathima N, Malini R, et al. Raman spectroscopy studies for diagnosis of cancers in human uterine cervix. *Vibrational Spectroscopy.* 2006;41(1):136-141.

41. Shaikh R, Dora TK, Chopra S, et al. In vivo Raman spectroscopy of human uterine cervix: exploring the utility of vagina as an internal control. *J Biomed Opt.* 2014;19(8):087001.

42. Mahadevan-Jansen A, Mitchell MF, Ramanujam N, Utzinger U, Richards-Kortum R. Development of a Fiber Optic Probe to Measure NIR Raman Spectra of Cervical Tissue In Vivo. *Photochemistry and Photobiology.* 1998;68(3):427-431.

43. Duraipandian S, Zheng W, Ng J, Low JJH, Ilancheran A, Huang Z. Effect of hormonal variation on in vivo high wavenumber Raman spectra improves cervical precancer detection. 2012:82140A-82140A.

44. Duraipandian S, Zheng W, Ng J, Low JJ, Ilancheran A, Huang Z. Non-invasive analysis of hormonal variations and effect of postmenopausal Vagifem treatment on women using in vivo high wavenumber confocal Raman spectroscopy. *Analyst.* 2013;138(14):4120-4128.

45. Kanter EM, Majumder S, Kanter GJ, Woeste EM, Mahadevan-Jansen A. Effect of hormonal variation on Raman spectra for cervical disease detection. *American Journal of Obstetrics and Gynecology.* 2009;200(5):512.e511-512.e515.

46. Vargis E, Brown N, Williams K, et al. Detecting biochemical changes in the rodent cervix during pregnancy using Raman spectroscopy. *Ann Biomed Eng.* 2012;40(8):1814-1824.

47. O'Brien CM, Herington JL, Brown N, et al. In vivo Raman spectral analysis of impaired cervical remodeling in a mouse model of delayed parturition. *Scientific reports.* 2017;7(1):6835.

48. Lieber CA, Mahadevan-Jansen A. Automated method for subtraction of fluorescence from biological Raman spectra. *Appl Spectrosc.* 2003;57(11):1363-1367.

49. Liang K-Y, Zeger SL. Longitudinal data analysis using generalized linear models. *Biometrika.* 1986;73(1):13-22.

50. Hanley JA, Negassa A, Edwardes MD, Forrester JE. Statistical analysis of correlated data using generalized estimating equations: an orientation. *American journal of epidemiology.* 2003;157(4):364-375.

51. Vargis E, Byrd T, Logan Q, Khabele D, Mahadevan-Jansen A. Sensitivity of Raman spectroscopy to normal patient variability. *J Biomed Opt.* 2011;16(11):117004.

52. Yoshida K, Jiang H, Kim M, et al. Quantitative Evaluation of Collagen Crosslinks and Corresponding Tensile Mechanical Properties in Mouse Cervical Tissue during Normal Pregnancy. *PloS one.* 2014;9(11):e112391.

53. Mandair GS, Morris MD. Contributions of Raman spectroscopy to the understanding of bone strength. *BoneKEy Rep.* 2015;4.

54. Gasior-Glogowska M, Komorowska M, Hanuza J, Ptak M, Kobielarz M. Structural alteration of collagen fibres--spectroscopic and mechanical studies. *Acta of bioengineering and biomechanics.* 2010;12(4):55-62.

55. Akins ML, Luby-Phelps K, Mahendroo M. Second harmonic generation imaging as a potential tool for staging pregnancy and predicting preterm birth. *J Biomed Opt.* 2010;15(2):026020.

56.     Yao W, Gan Y, Myers KM, Vink JY, Wapner RJ, Hendon CP. Collagen Fiber Orientation and Dispersion in the Upper Cervix of Non-Pregnant and Pregnant Women. *PLoS One.* 2016;11(11):e0166709.

57.     Sakamoto Y, Moran P, Bulmer JN, Searle RF, Robson SC. Macrophages and not granulocytes are involved in cervical ripening. *J Reprod Immunol.* 2005;66(2):161-173.

58.     Timmons BC, Mahendroo MS. Timing of neutrophil activation and expression of proinflammatory markers do not support a role for neutrophils in cervical ripening in the mouse. *Biol Reprod.* 2006;74(2):236-245.

59.     De Gelder J, De Gussem K, Vandenabeele P, Moens L. Reference database of Raman spectra of biological molecules. *Journal of Raman Spectroscopy.* 2007;38(9):1133-1147.

60.     Koyama Y, Takatsuka I, Nakata M, Tasumi M. Raman and infrared spectra of the all-trans, 7-cis, 9-cis, 13-cis and 15-cis isomers of β-carotene: Key bands distinguishing stretched or terminal-bent configurations form central-bent configurations. *Journal of Raman Spectroscopy.* 1988;19(1):37-49.

61.     Hata TR, Scholz TA, Pershing LK, et al. Non-Invasive Raman Spectroscopic Detection of Carotenoids in Human Skin. *J Invest Dermatol.* 2000;115(3):441-448.

62.     Wendremaire M, Goirand F, Barrichon M, Lirussi F, Peyronel C, Dumas M. Leptin prevents MMP activation in an in vitro model of myometrial inflammation. *Fundam Clin Pharmacol.* 2012;26.

63.     Wendremaire M, Mourtialon P, Goirand F, Lirussi F, Barrichon M, Hadi T. Effects of leptin on lipopolysaccharide-induced remodeling in an in vitro model of human myometrial inflammation. *Biol Reprod.* 2013;88.

64.     Wendremaire M, Bardou M, Peyronel C, Hadi T, Sagot P, Morrison JJ. Effects of leptin on lipopolysaccharide-induced myometrial apoptosis in an in vitro human model of chorioamnionitis. *Am J Obstet Gynecol.* 2011;205.

65.     Lui H, Zhao J, McLean D, Zeng H. Real-time Raman spectroscopy for in vivo skin cancer diagnosis. *Cancer Res.* 2012;72(10):2491-2500.

66.     Bergholt MS, Zheng W, Ho KY, et al. Fiberoptic confocal raman spectroscopy for real-time in vivo diagnosis of dysplasia in Barrett's esophagus. *Gastroenterology.* 2014;146(1):27-32.

Table 1. Patient demographics and outcome.

| Variable | |
|---|---|
| **Total patients (n)** | 68 |
| **Obstetric History** | |
| No prior pregnancies (n) | 28 |
| Prior pregnancies (n) | 40 |
| Prior vaginal deliveries (n) | 30 |
| **Pre-pregnancy BMI**[a] | |
| Mean (± SEM) | 29.3 (7.6) |
| Underweight/normal (<25) (n) | 19 |
| Overweight (25-30) (n) | 25 |
| Obese (30-35) (n) | 8 |
| Severely obese (35-40) (n) | 7 |
| Morbidly obese (BMI>40) (n) | 8 |
| **Obstetric outcome**[b] | |
| Delivered vaginally at term (n) | 32 |
| Delivered vaginally preterm (n) | 4 |
| C-section at term (n) | 25 |
| C-section preterm (n) | 5 |

[a]BMI was not available for one patient
[b]Outcome was not available for two patients

**Figure legends**

Figure 1. *In vivo* Raman spectroscopy of the cervix during pregnancy. A) Portable Raman spectroscopy system; B) Raman probe measurement from the cervix in vivo; C) Raman spectra from one patient over the course of her pregnancy and post-partum.

Figure 2. Computational model depicting how Raman spectra change over the course of pregnancy and post-partum. Shaded regions indicate spectral bands that exhibited significant changes throughout pregnancy: * indicates $p < 0.05$ over the course of pregnancy, # indicates $p < 0.05$ when comparing early pregnancy (<20 weeks) and post-partum, and ‡ indicates $p < 0.05$ when comp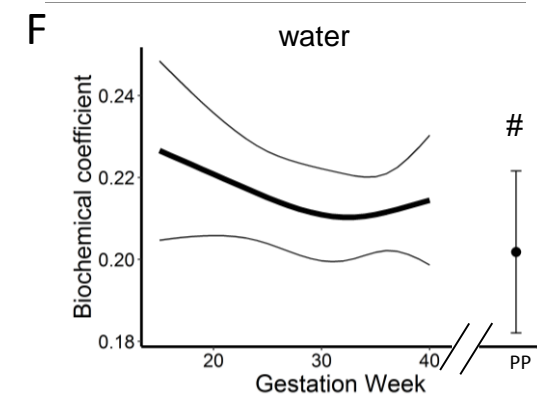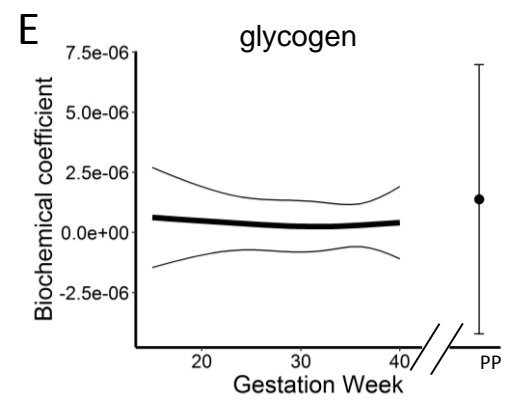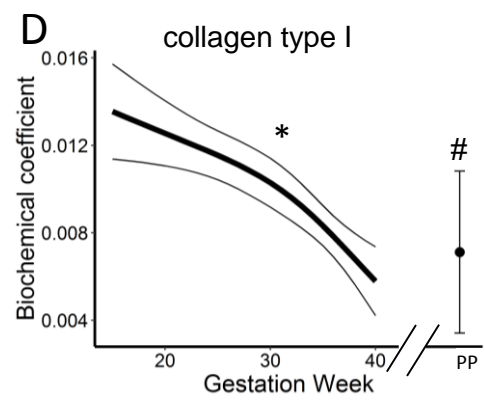aring late pregnancy (>37 weeks) to post-partum measurements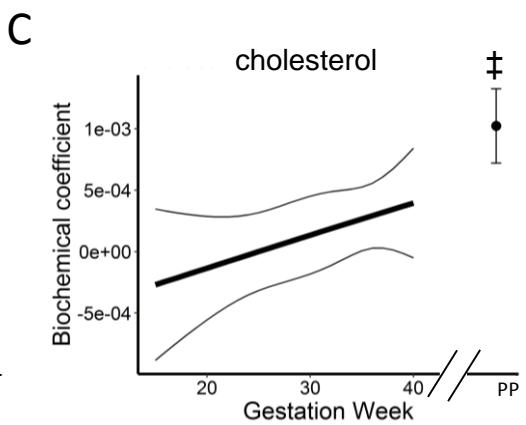 ($p < 0.05$). Spectral regions associated with specific molecular peaks are labeled as such: a- actin, ATP- adenosine triphosphate, b-blood, car-carotenoids, chol-cholesterol, col- collagen type I, g-glucose, and w-water.

Figure 3. *In vivo* Raman peak ratios displayed in a general linear model over the course of pregnancy. * indicates $p < 0.005$ over the course of pregnancy, # indicates $p < 0.05$ when comparing early pregnancy (<20 weeks) and post-partum, and ‡ indicates $p < 0.05$ when comparing late pregnancy (>37 weeks) to post-partum measurements.

Figure 4. Non-negative least squares biochemical model of *in vivo* Raman spectra. A-F) Raman spectra from pure biochemical components (actin, blood, cholesterol, collagen type I, glycogen, and water) and G) a representative cervix tissue spectrum (blue) with its model fit (pink) and residual (green).

Figure 5. Biochemical contributions over the course of pregnancy. The fitted component coefficient for actin (A), blood (B), cholesterol (C), collagen type 1 (D), glycogen (E), and water (F), plotted against gestation week (mean and 95% confidence interval). * indicates $p<0.005$ over the course of pregnancy, # indicates $p<0.05$ when comparing early pregnancy (<20 weeks) and post-partum, and ‡ indicates $p<0.05$ when comparing late pregnancy (>37 weeks) to post-partum measurements.

Figure 6. Computational model comparing Raman spectral changes as a function of gestation week and post-partum in A) nulliparous (n=29) vs. parous patients (n=37), B) patients with normal (model set to BMI=25, n=51) and high (model set to BMI=40, n=15) body mass index. Gray bars highlight areas that underwent significant change over pregnancy or post-partum, * and # indicate that patient variable had significant effect on spectral region over the course of pregnancy and post-partum repair, respectively.
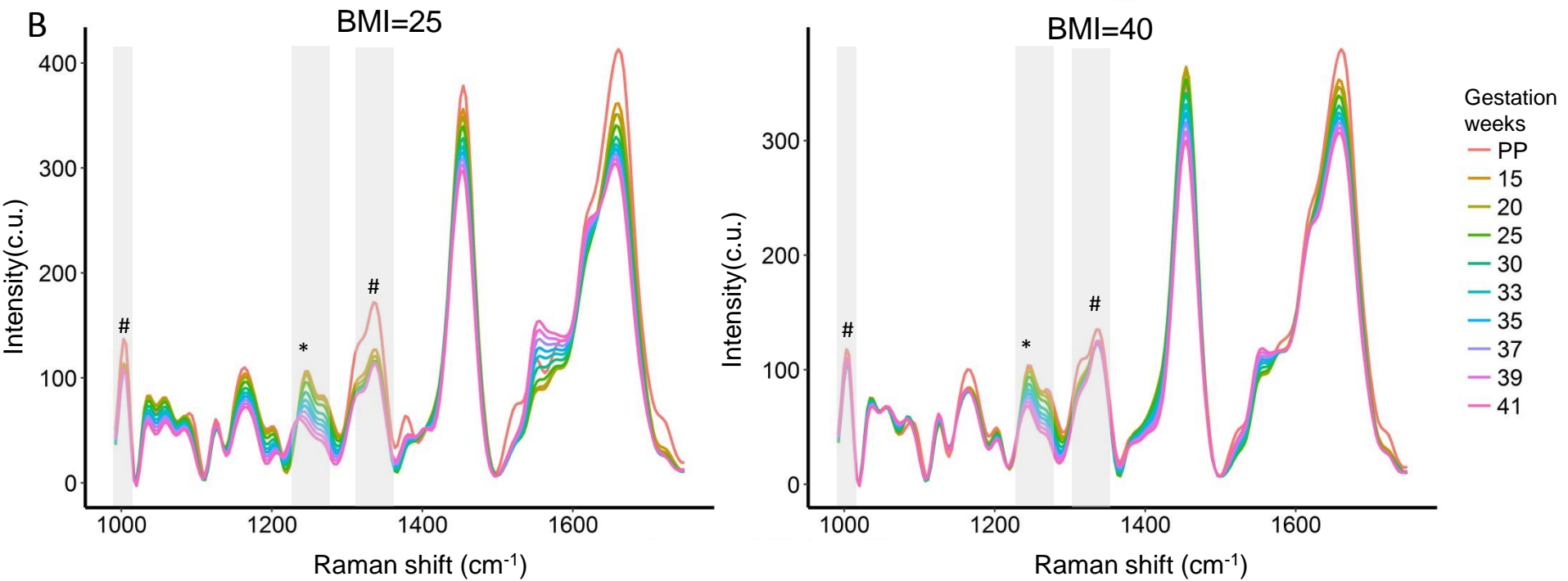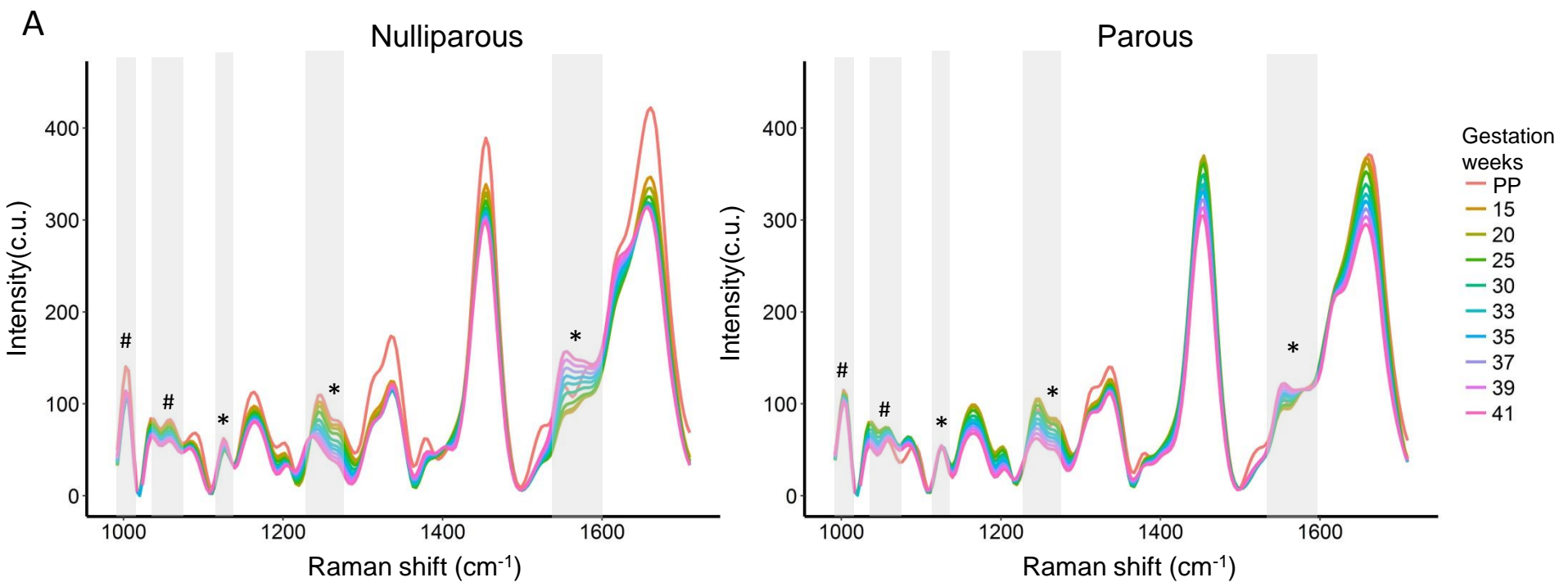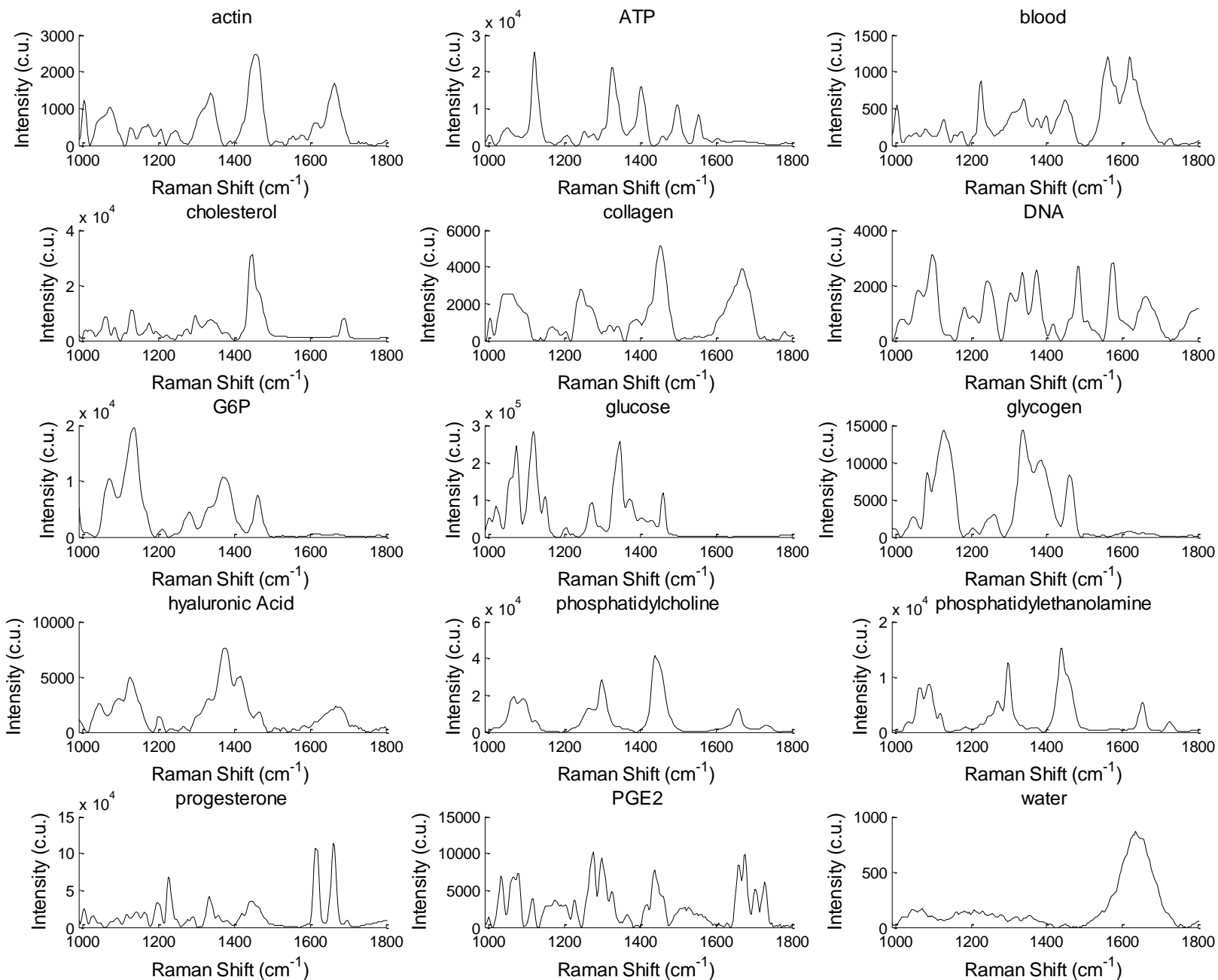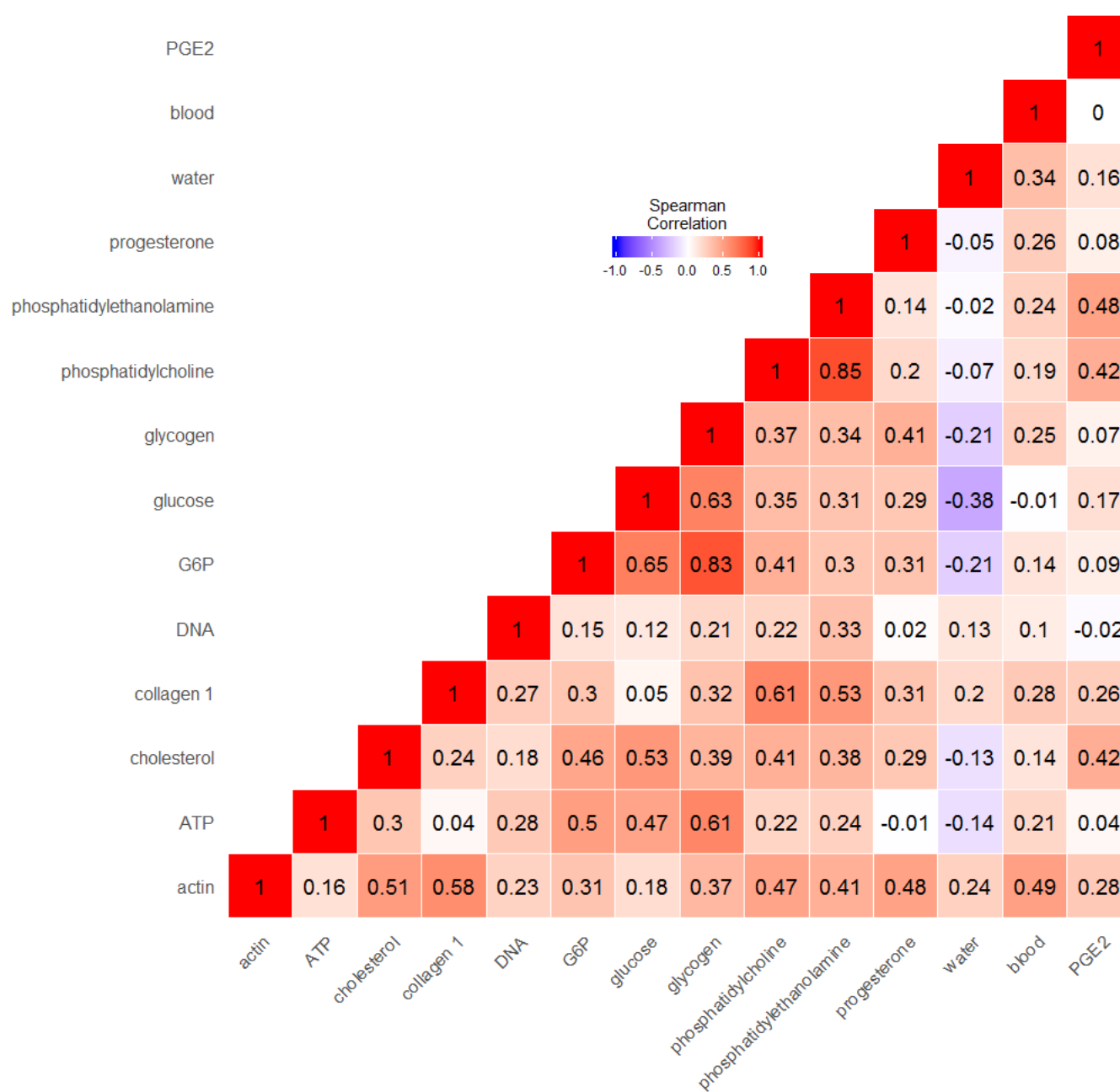
A — actin

B — blood

C — cholesterol

D — collagen type I

E — glycogen

F — water

**A**

Nulliparous

Parous

**B**

BMI=25

BMI=40

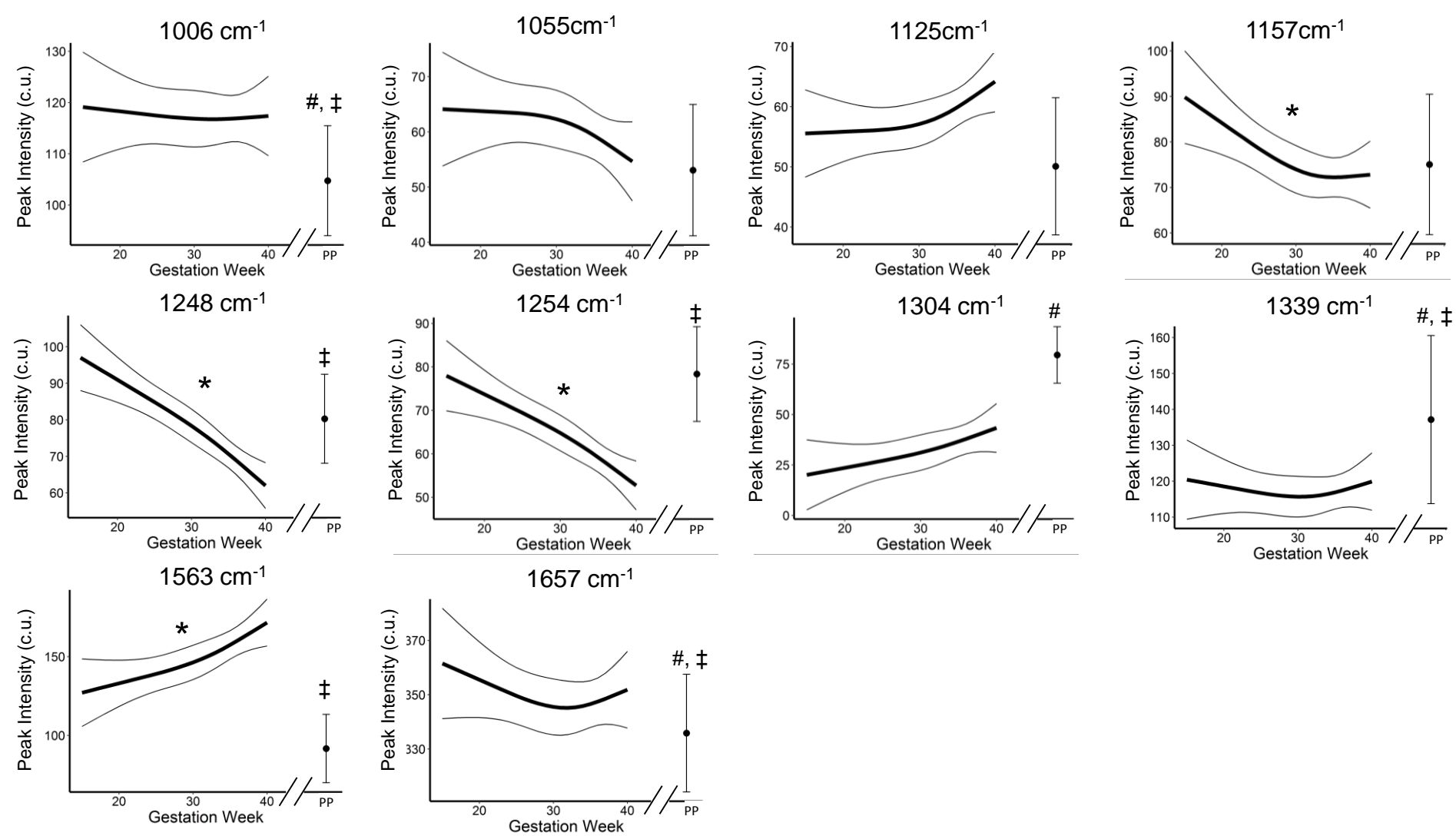Gestation weeks: PP, 15, 20, 25, 30, 33, 35, 37, 39, 41
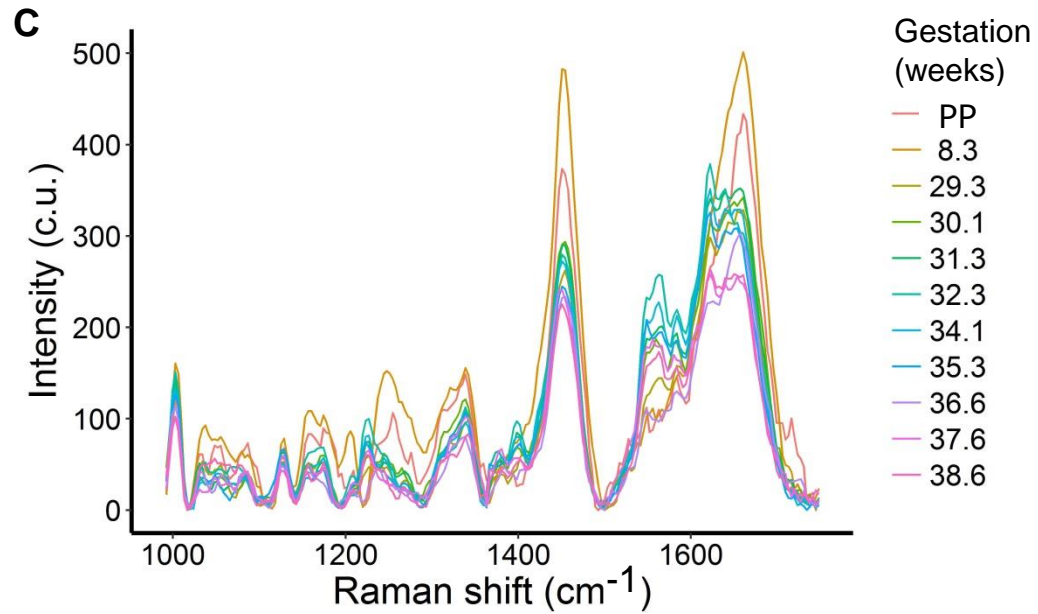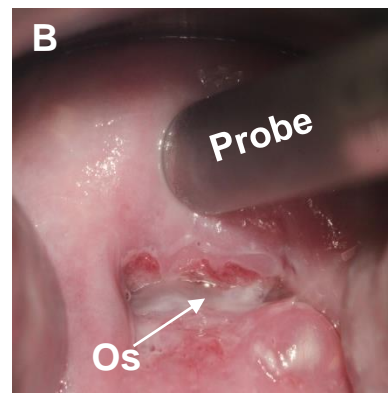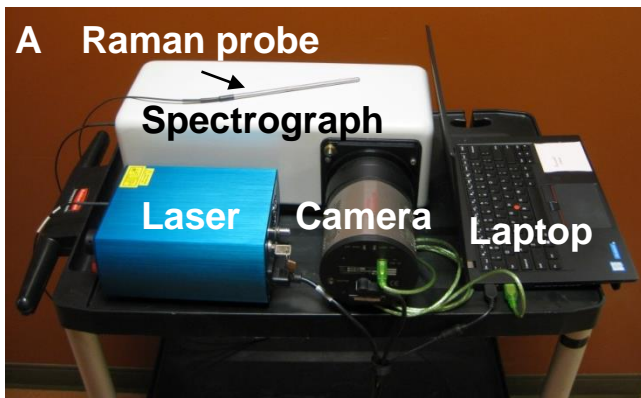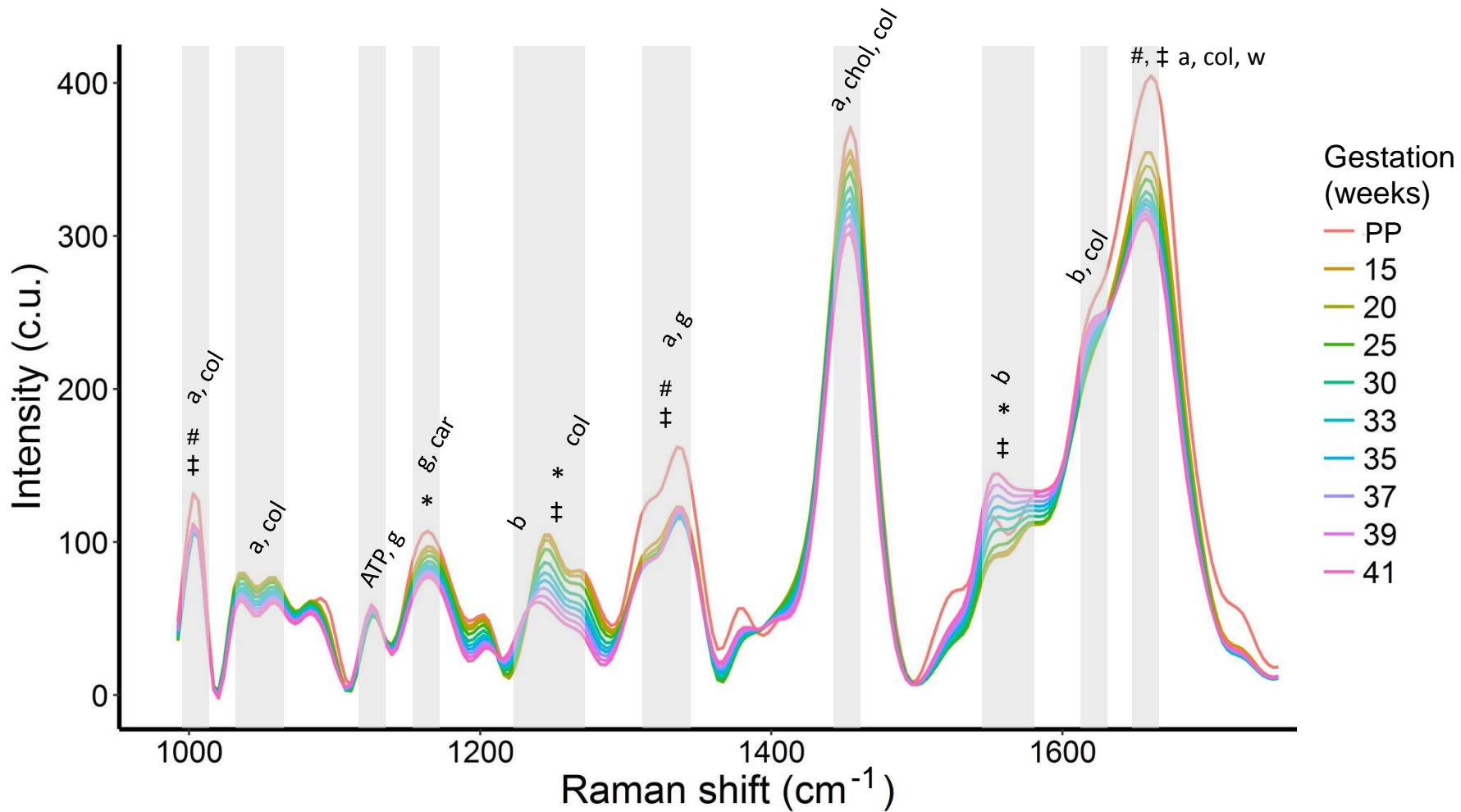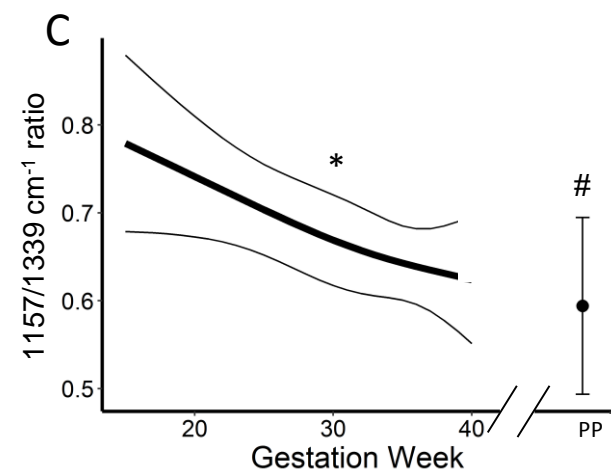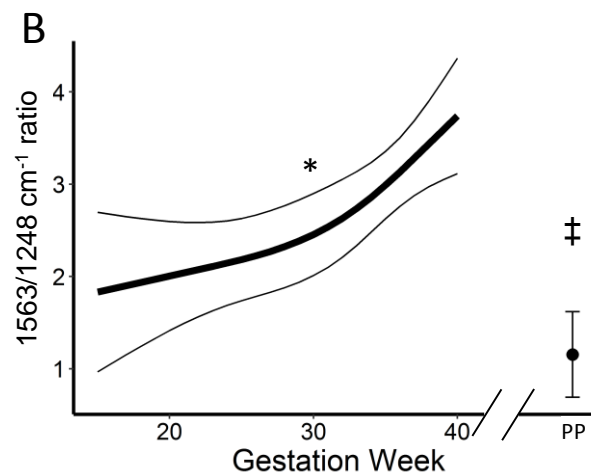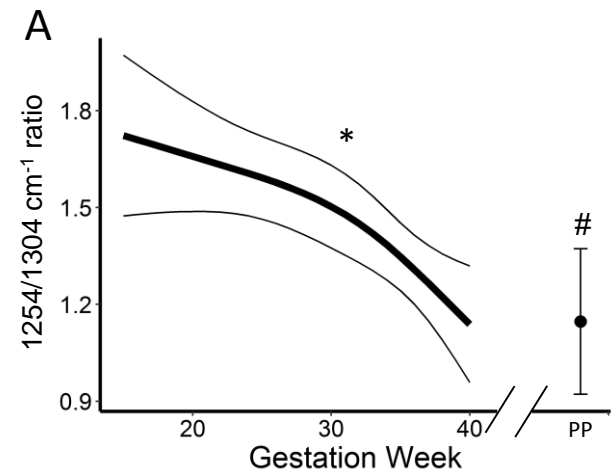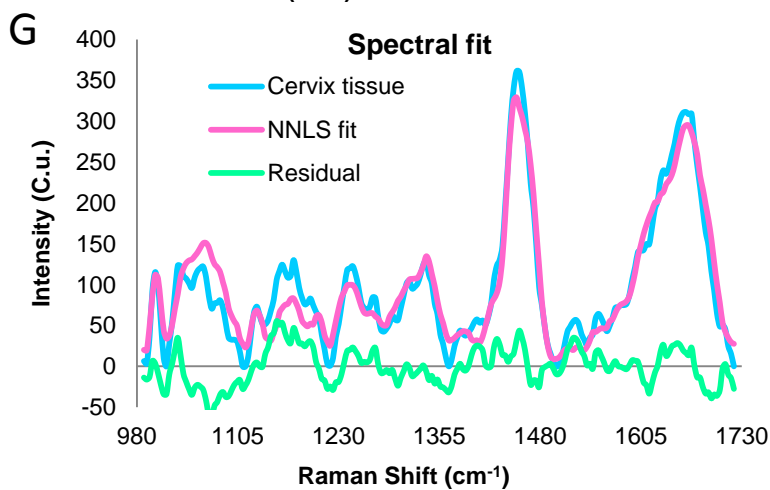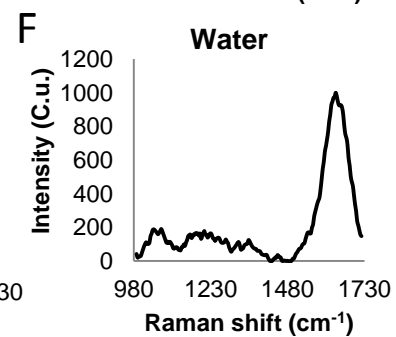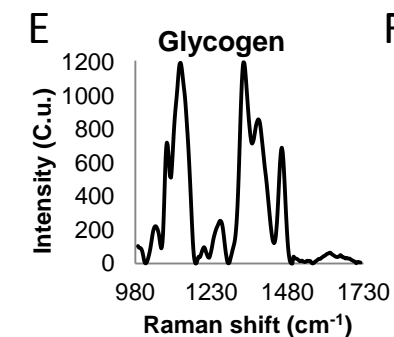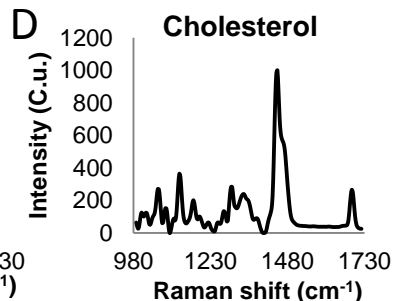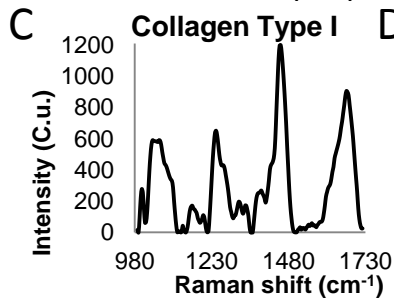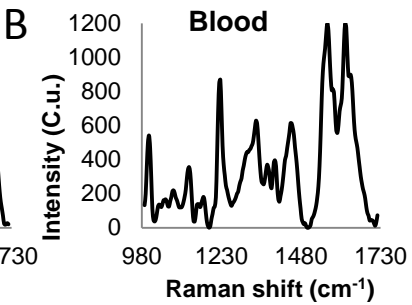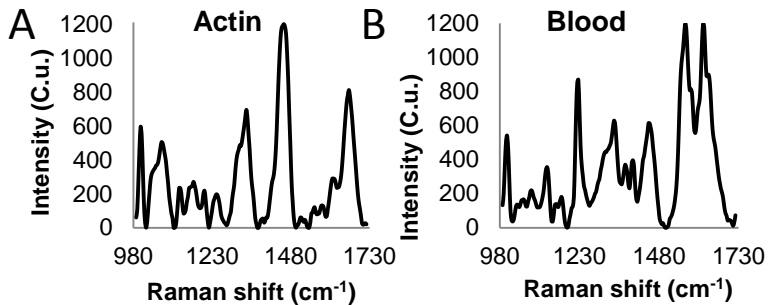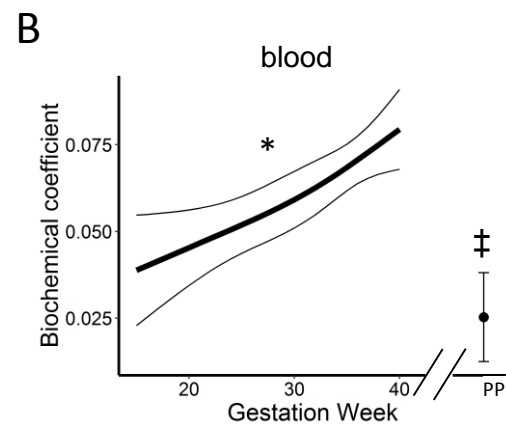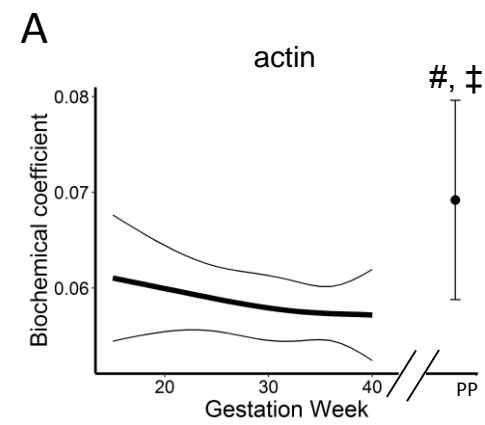
# Supplementary figures

**Supplemental Figure 1.** Raman spectra of pure chemicals that were evaluated as potential least squares model inputs.

**Supplemental Figure 2.** Correlation coefficient matrix comparing similarity between pure chemical Raman spectra.

**Supplemental Figure 3.** Raman spectral peak intensities over the progression of pregnancy. * indicated $p<0.005$ over the course of pregnancy, # indicates $p<0.05$ when comparing early pregnancy (<22 weeks) and post-partum, and ‡ indicates $p<0.05$ when comparing late pregnancy (>37 weeks) to post-partum measurements. (Mean and 95% confidence interval)
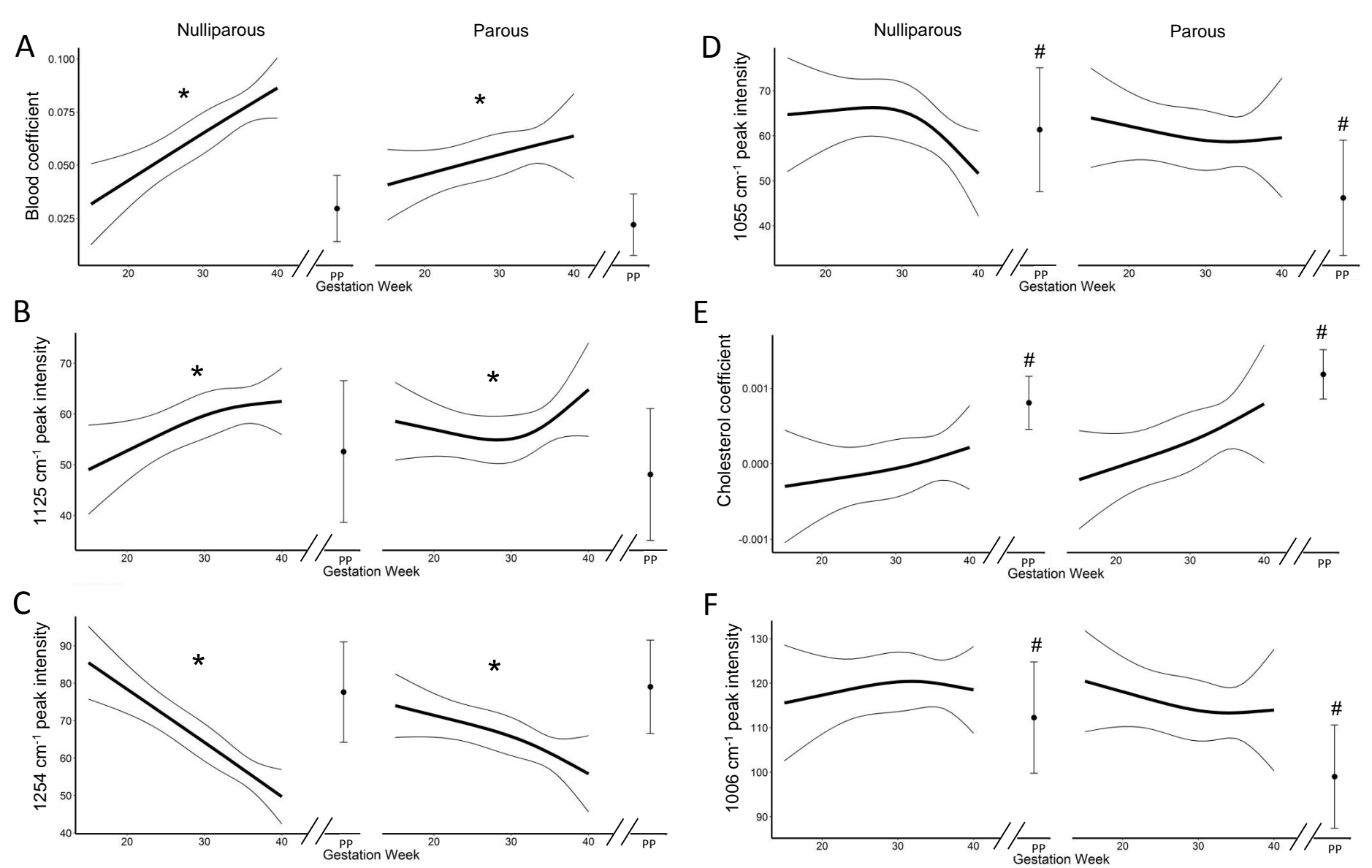
**Supplemental Figure 4.** Non-negative least squares coefficients and Raman spectral peak intensities that have significant differences during pregnancy or post-partum based on patient parity. * indicates significant differences (p<0.05) due to parity over the course of pregnancy, # indicates significant differences (p<0.05) due to parity when comparing post-partum measurements. (Mean and 95% confidence interval)
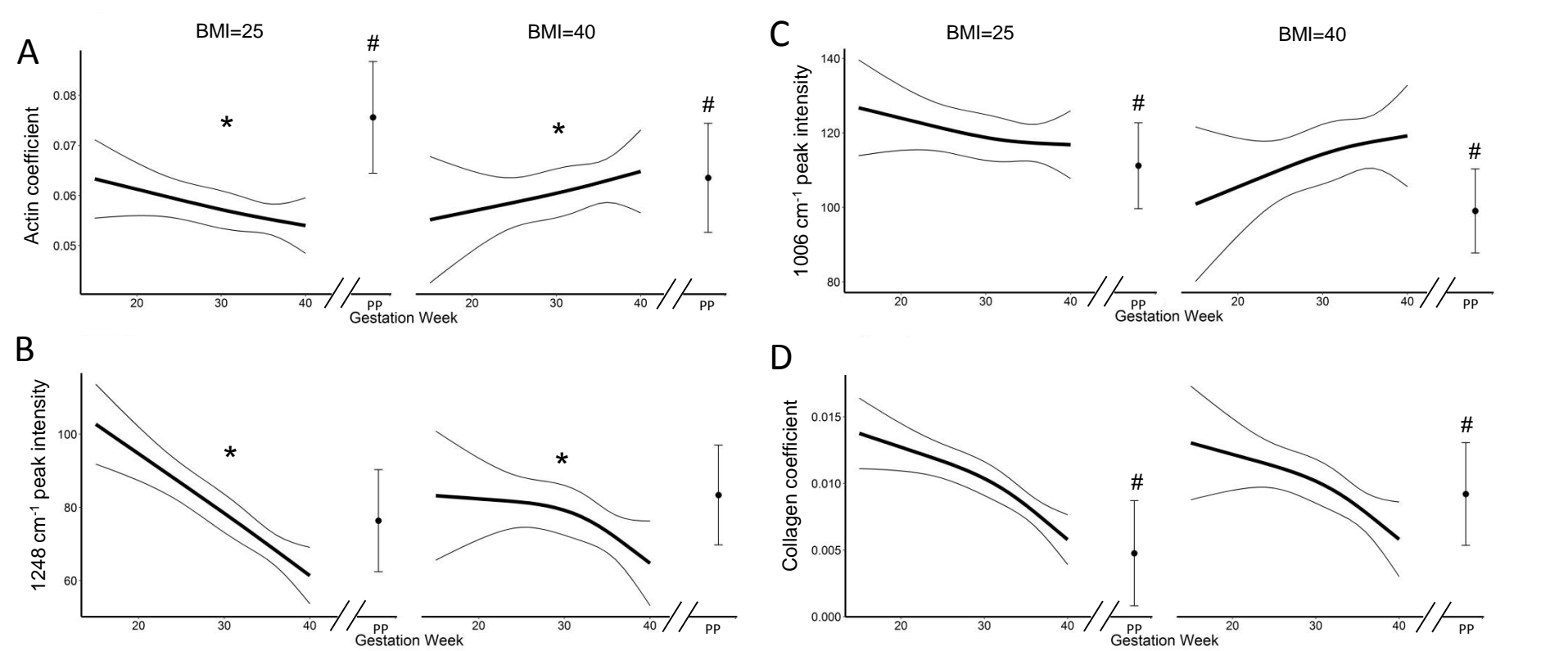
**Supplemental Figure 5.** Non-negative least squares coefficients and Raman spectral peak intensities that have significant differences based on patient body mass index. * indicates significant differences (p<0.05) due to BMI over the course of pregnancy, # indicates significant differences (p<0.05) due to BMI when comparing post-partum measurements. (Mean and 95% confidence interval)